An extended formulation of the Maximum Likelihood Estimation algorithm. Application to space-time adaptive processing.

Jean-François DEGURSE[1,2], Laurent SAVY[1], Rémi PERENON[1], Sylvie MARCOS[2]

[1]Electromagnetism and Radar Department, ONERA
Palaiseau, FRANCE
email : jean-francois.degurse@onera.fr, laurent.savy@onera.fr

[2]L2S, CNRS-SUPELEC-Univ Paris-Sud
Gif-sur-Yvette, France
email : sylvie.marcos@lss.supelec.fr

Abstract: *This paper proposes an extended version of the Maximum Likelihood Estimation Detector (MLED) that can operate in severe heterogeneous environment for slow moving target detection in ground clutter using space-time adaptive processing (STAP). Unlike the MLED, the extended version called STOP-BAND APES does not suffer from the high Doppler resolution properties of the MLED leading to severe extra computational burden. Performances are illustrated on realistic synthetic data.*

1. Introduction

Classical space-time adaptive processing (STAP) detectors are strongly limited when facing a severe non stationary environment (heterogeneous clutter or a high target density). Indeed in this case representative target free training data are no longer available. To overcome this problem, the Maximum Likelihood Estimation Detector (MLED), detailed in [1], only operates with the data in the cell under test. However, this is a high resolution method, thus requiring an important oversampling. In this paper, an extended version of the MLED is proposed that prevents this oversampling. Its performances are demonstrated on realistic synthetic data.

2. Extended formulation of the MLED: STOP-BAND APES

Consider a radar antenna made of N sensors that acquire Mp snapshots. For a more compact formulation, we adopt the following formalism:

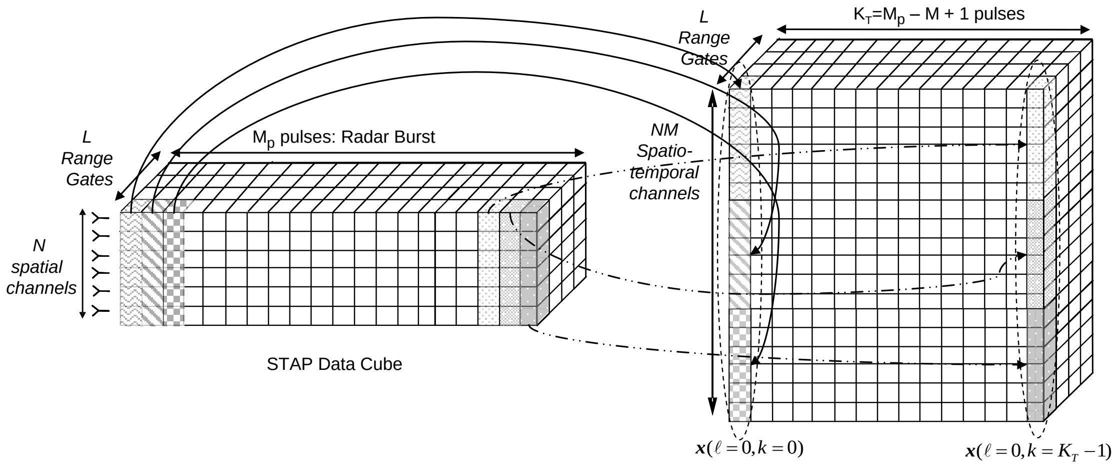

Figure 1 : Space-time datacube and data re-organisation

The different data vectors $\boldsymbol{x}(\ell,\{k\})$ for range cell ℓ and all the pulses $\{k\}=0:K_T-1$ are concatenated to form a data matrix $\boldsymbol{X}(\ell)$: $\boldsymbol{X}(\ell)=[\boldsymbol{x}(\ell,0)\ \boldsymbol{x}(\ell,1)\cdots\boldsymbol{x}(\ell,K_T-1)]$. From now, we will forget the subscript ℓ , given that the MLED processing works independently in each range cell. We adopt the same model as defined in [1]:

$$\boldsymbol{X}=\alpha\,\boldsymbol{s}_s\boldsymbol{s}_t^T+\boldsymbol{N} \tag{1}$$

With $\boldsymbol{s}_s$ the spatio-temporal steering vector (length NM), $\boldsymbol{s}_t$ the temporal steering vector (length K_t) and $\boldsymbol{N}$ the noise matrix. In [1], Aboutanios and Mulgrew proposed a new detector called maximum likelihood estimation detector (MLED), derived from the APES filter [2], which uses only primary data set as training data. The problem is stated as follows:

$$\min_{w,\alpha}\left\{(\boldsymbol{w}^H\boldsymbol{X}-\alpha\boldsymbol{s}_t)(\boldsymbol{w}^H\boldsymbol{X}-\alpha\boldsymbol{s}_t)^H\right\}\qquad \text{s.t.}\qquad \boldsymbol{w}^H\boldsymbol{s}_s=1 \tag{2}$$

The solution obtained is by $\boldsymbol{w}=\dfrac{\boldsymbol{Q}^{-1}\boldsymbol{s}_s}{\boldsymbol{s}_s^H\boldsymbol{Q}^{-1}\boldsymbol{s}_s}$ and $\alpha=\dfrac{\boldsymbol{w}^H\boldsymbol{X}\boldsymbol{s}_t^*}{\boldsymbol{s}_t^T\boldsymbol{s}_t^*}$ (3)

where $\boldsymbol{Q}=\boldsymbol{R}-\boldsymbol{g}\boldsymbol{g}^H$ is the signal free covariance matrix (4)

$\boldsymbol{g}=\dfrac{\boldsymbol{X}\boldsymbol{s}_t^*}{\boldsymbol{s}_t^T\boldsymbol{s}_t^*}$ and $\boldsymbol{R}=\dfrac{\boldsymbol{X}\boldsymbol{X}^H}{\boldsymbol{s}_t^T\boldsymbol{s}_t^*}$ is the estimated data covariance matrix

Combining (2) and (3) it follows:

$$\boldsymbol{w}^H\left(\boldsymbol{X}-\boldsymbol{X}\frac{\boldsymbol{s}_t^*\boldsymbol{s}_t^T}{\boldsymbol{s}_t^T\boldsymbol{s}_t^*}\right)\left(\boldsymbol{X}-\boldsymbol{X}\frac{\boldsymbol{s}_t^*\boldsymbol{s}_t^T}{\boldsymbol{s}_t^T\boldsymbol{s}_t^*}\right)^H\boldsymbol{w}=\boldsymbol{w}^H\boldsymbol{X}(\boldsymbol{Id}-P_{//})(\boldsymbol{Id}-P_{//})^H\boldsymbol{X}\boldsymbol{w}$$

where $\mathbf{P}_{//}$ is the projector into the target signal subspace: $\boldsymbol{P}_{//}=\dfrac{\boldsymbol{s}_t^*\boldsymbol{s}_t^T}{\boldsymbol{s}_t^T\boldsymbol{s}_t^*}=\dfrac{\boldsymbol{s}_t^*\boldsymbol{s}_t^T}{K_t}$.

The problem (2) can then be recognized as a minimization of the interference plus noise energy outside the subspace spanned by the target:

$$\min_{\boldsymbol{w}}\left\{\boldsymbol{w}^H\boldsymbol{X}(\boldsymbol{Id}-P_{//})(\boldsymbol{Id}-P_{//})^H\boldsymbol{X}\,\boldsymbol{w}\right\}\qquad \text{s.t.}\qquad \boldsymbol{w}^H\boldsymbol{s}_s=1 \tag{5}$$

The solution is still $\boldsymbol{w}=\dfrac{\boldsymbol{Q}^{-1}\boldsymbol{s}_s}{\boldsymbol{s}_s^H\boldsymbol{Q}^{-1}\boldsymbol{s}_s}$, but with the more general form for Q:

$$\mathbf{Q}=\frac{\mathbf{X}\mathbf{X}^H}{\mathbf{s}_t^T\mathbf{s}_t^*}-\frac{1}{K_t}\mathbf{X}\mathbf{P}_{//}\mathbf{X}^H$$

This latest formulation allow to overcome one major drawback of the MLED method for our application. The MLED has indeed a high frequency resolution due to the sharpness of the projection $(\boldsymbol{Id}-\boldsymbol{P}_{//})$ with $\boldsymbol{P}_{//}=\dfrac{\boldsymbol{s}_t^*\boldsymbol{s}_t^T}{\boldsymbol{s}_t^T\boldsymbol{s}_t^*}$ (solid curve, Fig. 2). This is a problem because it requires a strong oversampling to be sure to remove the signal of interest from the covariance matrix $\mathbf{R}$, and so leads to an important increase of the computing load. In order to avoid this problem, we propose a new detector called stop-band MLED. The minimization is made like in (5) but using a projector $\mathbf{P}_{//}$ that spanned an extended subspace around the Doppler frequency f_0 under test. For instance, two half-cells adjacent can be added into the space spanned by $\mathbf{P}_{//}$, letting

$$\boldsymbol{S}_t = [\boldsymbol{s_t}(f_0 - \frac{1}{2K_t}), \boldsymbol{s_t}(f_0), \boldsymbol{s_t}(f_0 + \frac{1}{2K_t})] \qquad \text{and} \qquad \boldsymbol{P}_{//} = \boldsymbol{S}_t^{*}(\boldsymbol{S}_t^{\boldsymbol{T}}\boldsymbol{S}_t^{*})^{-1}\boldsymbol{S}_t^{\boldsymbol{T}}$$

The sharpness and effectiveness of the cancellation of the target signal around f_0 is characterized by the projector's frequency response which is, for a signal $\boldsymbol{X}$ at frequency f ($\boldsymbol{X} = \boldsymbol{s}_t^{\boldsymbol{T}}(f)$) :

$$\tilde{P}_{\perp}(f) = \left[\boldsymbol{s}_t^{\boldsymbol{T}}(f)\left(\boldsymbol{Id} - \boldsymbol{P}_{//}\right)\right]\frac{\boldsymbol{s}_t^{*}(f)}{\boldsymbol{s}_t^{\boldsymbol{T}}(f)\boldsymbol{s}_t^{*}(f)} = 1 - \boldsymbol{s}_t^{\boldsymbol{T}}(f_1)\frac{\boldsymbol{P}_{//}}{K_T}\boldsymbol{s}_t^{*}(f)$$

Fig. 2 shows that building a projector with two adjacent cells is not enough to correctly remove the signal in the cell under test (about only 20 dB attenuation). However, attenuations over 50 dB for all signal located in the same frequency cell as the cell under test are obtained by using two adjacent half-cells. We can conclude that the use of half-cells is necessary.

Nevertheless, compared to the MLED, the STOP-BAND APES does not require oversampling from the Doppler resolution for the calculation and the application of the STAP filter. (Although a zero-padding by a factor 2 will still be required for the Fourier transform to access the signals $\boldsymbol{g}_i$ that have to be evaluated every half-resolution cells for the creation of the projector).

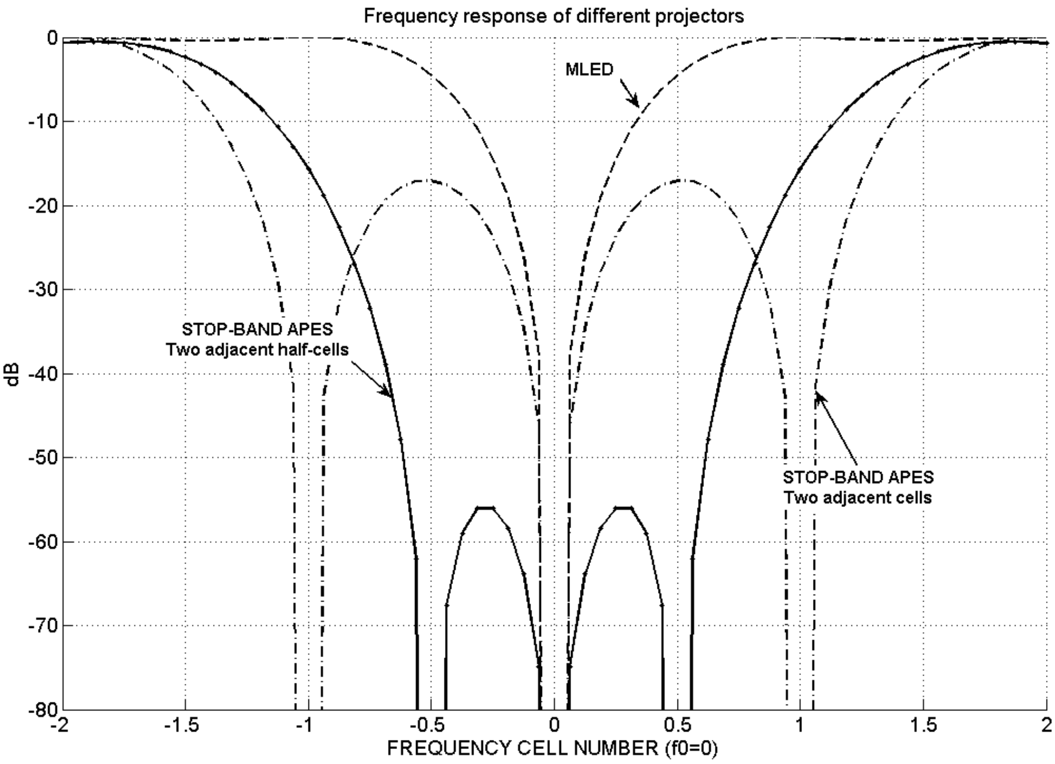

Figure 2 : Spectral response of three projectors.

Regular MLED: $S = s_t$ (dash curve), STOP-BAND APES with two adjacent half-cells (solid curve), STOP-BAND APES with two adjacent cells (dot-dash curve)

3. Performances

We present the performances of this algorithm on realistic synthetic data obtained with ONERA's simulator using an AMSAR like antenna. The AMSAR antenna is an active multi-channel nose radar antenna for combat aircraft composed of 8 sub-arrays. Configuration used for data simulation is shown in Tab. 1 and illustrated on Fig. 3.1 and Fig 3.2.

AIRCRAFT PARAMETERS		MODE PARAMETERS	
Speed	180m/s	PRF	2000 Hz
Height	10 000 feet	Azimut Scan angle	30°
RADAR PARAMETERS		Elevation Scan angle	-3°
Frequency Band	X	Range domain	37.5-75 km
Beamwidth oreceive (scan angle)	≅ 4°	SNR at 75 km	16 dB

Table 1. Data configuration

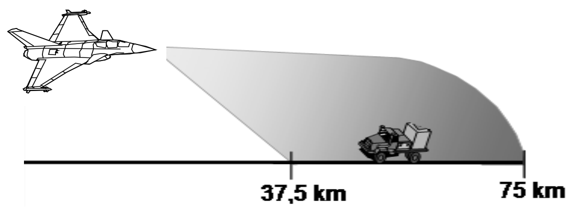

Figure 3.1 : Scene illustration of a combat aircraft radar in a air-to-ground mode and

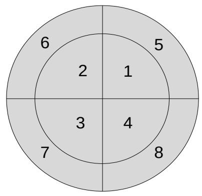

Figure 3.2 : AMSAR antenna splitting (8t subarrays)

On Fig. 4, the classical sum channel output is shown. One can cleary see that without any filtering, detection is impossible at speeds between -6 $m.s^{-1}$ and +6 $m.s^{-1}$. Note that range values starts at 37.5 km, beginning of range domain (Fig 3.1).

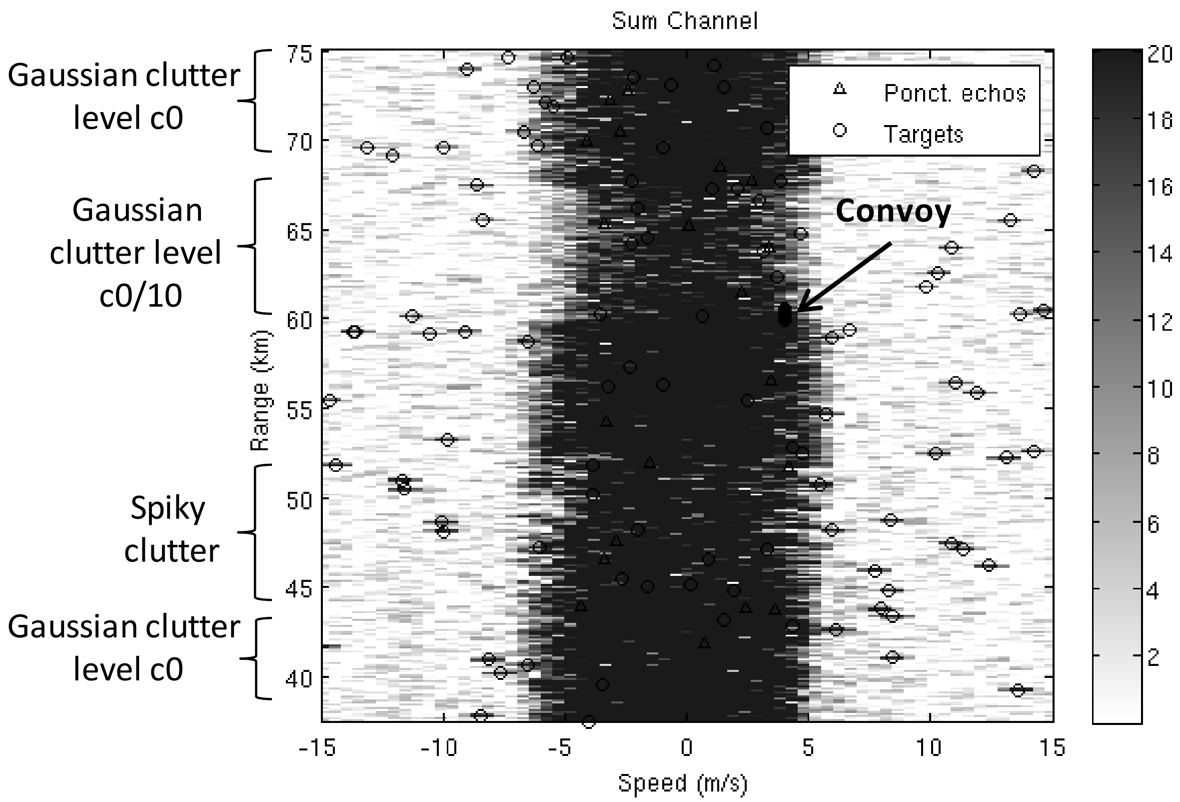

Figure 4: Range-speed map of the sum channel with the test data. Targets having a low speed (e.g convoy), less than +/- 6 $m.s^{-1}$ can't be detected with a classic Doppler filter.

The following results have been obtainded without oversampling. For MLED and STOP-BAND APES, only data within the range cell under test is used. We compare these methods with classical STAP FIR filters, [3], in which covariance matrix is estimated by mean over 10 range cells with 2 guard cells.

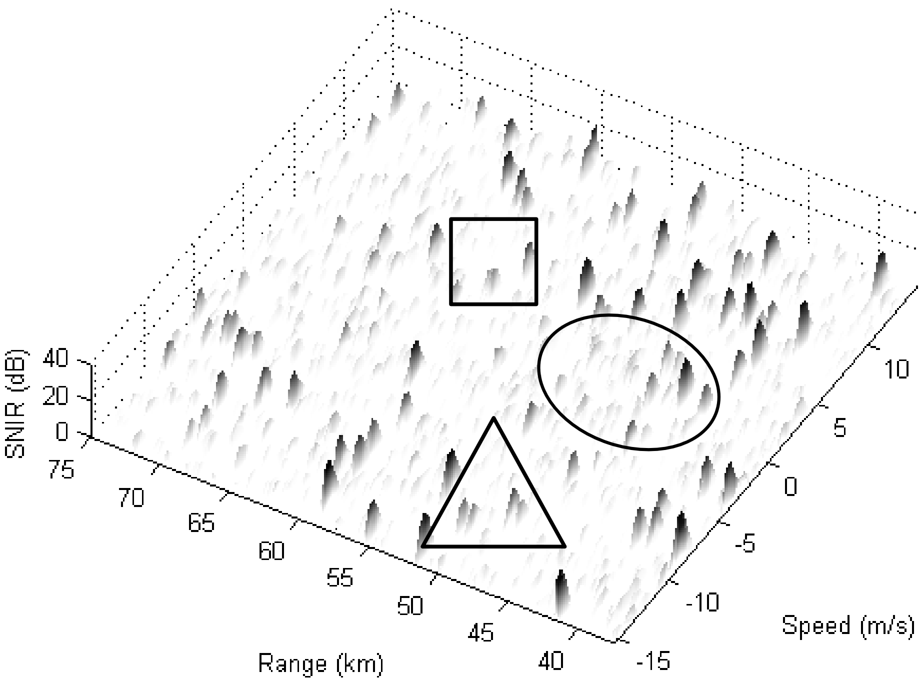

Figure 5: Range-speed map with classical FIR filters using 10 range cells. Square box points the convoy, triangle box shows high density target zone, and spiky clutter is contained in the oval form.

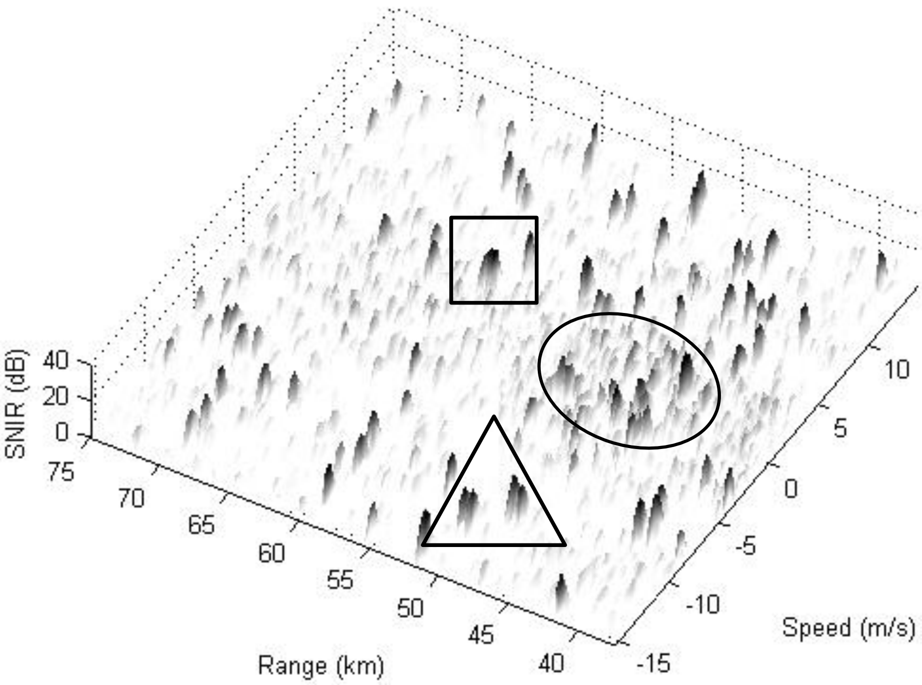

Figure 6: Range-speed map with APES STOP-BAND method using the cell under test. Square box points the convoy, triangle box shows high density target zone and spiky clutter is contained in the oval form.

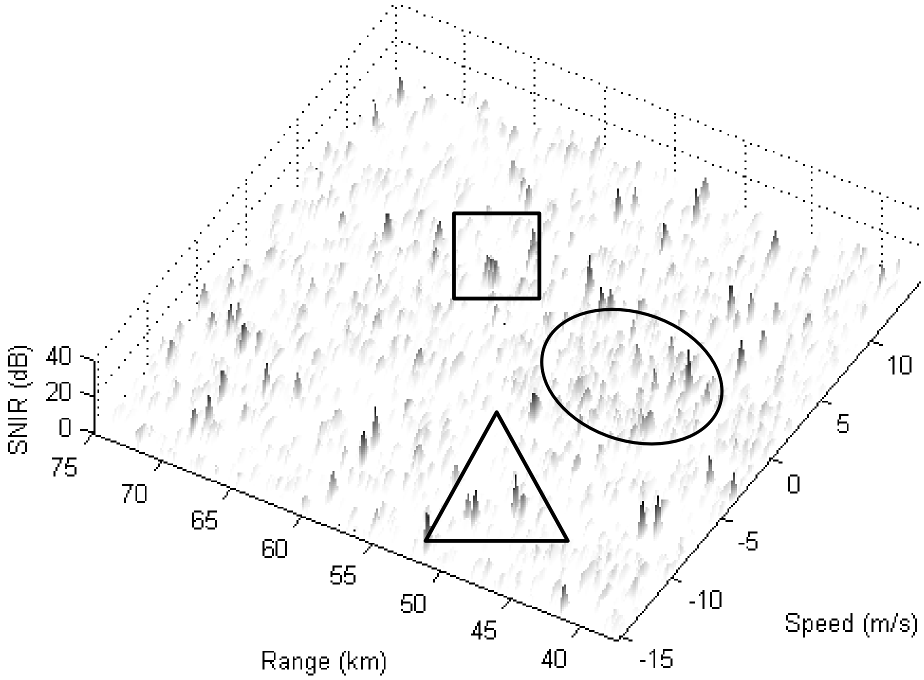

Figure 7: Range-speed map with MLED algorithm using the cell under test. Square box points the convoy, triangle box shows high density target zone and spiky clutter is contained in the oval form.

Fig.5, shows that FIR filtering performs very well in removing clutter. However, due to the use of adjacent range cells for clutter covariance matrix estimation, convoy as well as targets located in high density target areas are also mitigated. By not using training data from adjacent range cells, STOP-BAND APES does not remove convoys or targets in high density targets area (Fig. 6), but it fails to correctly suppressed the spiky clutter (because APES is basically an amplitude estimator). Finally, on Fig 7, it is shown that the MLED is unable to detect targets that are not exactly centered in a Doppler cell if no oversampling is used.

4. Conclusion

In this paper, we presented an alternative approach to classical adaptive processing, aiming to use only data of the cell under test. This approach is particularly well suited to the case of heavily heterogeneous environments such as non-stationary clutter or, in our example, high density of targets. The proposed method is an extension of the detector MLED. It prevents the high computationnal load of the MLED detector, due to its intrinsic hyper-resolution Doppler properties. The application of the proposed method on realistic data has proven its effectiveness. Work is ongoing to solve the problem of false alarm when facing spiky clutter, using correlation between Doppler and angular position for clutter echos.

References:

[1] E. Aboutanios, B. Mulgrew, “A STAP algorithm for radar target detection in heterogeneous environments”, *2005 IEEE/SP 13th Workshop on Statistical Signal Processing*, July 2005, pp 966-971.

[2] J. Li, P. Stoica, “A new derivation of the APES filter“, *IEEE Signal Processing Letters*, August 1999, 6 Issue:8 : 205-206.

[3] R. Klemm, “A STAP overview“, *IEEE Aerospace and Electronic Systems Magazine*, Vol 19, no. 1, pp19-35, Jan 2004